Physics – Uspekhi **40** (3) 257 – 272 (1997)

REVIEWS OF TOPICAL PROBLEMS PACS numbers: **36.20.–r**, **68.65.+g**, **78.20.Fm**, **78.66.–w**

Orientational order in polymer surface layers

A E Grishchenko, A N Cherkasov

Contents

1. **Introduction** 257
2. **Theoretical and methodological basis of surface birefringence studies** 258
   2.1 The theory of surface birefringence in polymer films; 2.2 Types of orientational order in surface layers; 2.3 Some aspects of the experimental technique
3. **Optical anisotropy and structural patterns of surface layers** 259
   3.1 Orientational order in surface layers of amorphous polymers; 3.2 Orientational order distribution across the film thickness; 3.3 The equivalent surface layer; 3.4 Effect of supports on the surface optical properties of polyparaxylylene
4. **Properties and structure of surface layers in epoxypolymer networks** 262
   4.1 Thickness and orientation of surface layers; 4.2 The role of kinetic effects in the formation of surface anisotropy
5. **Formation of surface layers in block-copolymers** 264
   5.1 Surface optical properties of polyether-based ureourethane; 5.2 Specific surface properties of two-component copolymers; 5.3 Methods for the formation of surface layers
6. **Orientational effects related to the formation of polymer membranes from solutions** 267
   6.1 General information; 6.2 The oblique incidence method in a study of membrane structure and formation kinetics; 6.3 Orientational order in the structure of polymer membranes
7. **Conclusions** 270

References 271

Abstract. The most important data from birefringence measurements on the structure, optical anisotropy, and formation kinetics of polymer surface layers are reviewed.

1. Introduction

Investigations into the mechanical properties of various substances have demonstrated that their quantitative characteristics are essentially dependent on the sample size. This can be accounted for by different local properties of matter in the surface layers and in the bulk. Evidently, the effect of the surface layers on averaged physical properties and their contribution to the characteristics of the sample as a whole increase with decreasing size (or film thickness). This phenomenon has been called the scale (or size) effect [1 – 12].

Naturally, this effect is apparent in polymer studies because the surface properties of polymer materials are responsible for many of their macroscopic parameters.

Surface properties include both the chemical composition of surface layers and their physical structure (specifically, orientational order in polymer chains). Surface layers of a polymer body are not only those separating it from the surrounding gaseous or liquid medium, they also line pores and cracks in the thick of the body and form the boundary between the polymer and the filler [7].

Surface properties of polymer materials arise due to the system's tendency to minimal interphase energy and depend on the mobility of molecular chains [13, 14]. The thickness of a layer whose properties differ from those in the remaining volume is related to the mode in which the surface is formed and varies considerably.

There is no universal approach to the study of surface properties of polymers and other substances with surface layers of different thicknesses and chemical composition. The available physical methods provide but limited information about the structure of surface layers. As a rule, different methods have to be combined to comprehensively characterize surface properties.

The surface orientation of anisotropic elements in polymer chains is currently studied by the birefringence technique (BT) which records polarized light passing through a film at an angle differing from the right angle [9, 15]. In 1930, McNally and Sheppard [16] found that cellulose acetate films are optically isotropic when a light beam falls normally on their surface but exhibit birefringence when the same beam falls at an angle. Later, Stein [15] explained this phenomenon as being due to the orientation of polymer chains and suggested an optical method to determine the type of orientation using BT measurements at two fixed angles. This method allowed orientational order to be characterized by three orthogonal refractive indices. A N Cherkasov et al. [9] modified the method of Stein to obtain more detailed information about orientational order in polymer materials. Specifically, BT was used to probe optical anisotropy of surface layers in a wide thickness range; the results confirmed its superiority over other approaches [9, 10].

A E Grishchenko St. Petersburg State University, 198904 Petrodvorets, St. Petersburg, Russia
A N Cherkasov State Research Institute for Highly Pure Biomaterials ul. Pudozhskaya 7, 197110 St. Petersburg, Russia

Received 21 March 1994, revised 4 November 1996
Uspekhi Fizicheskikh Nauk **167** (3) 269 – 285 (1997)
Translated by Yu V Morozov; edited by A I Yaremchuk

Angular BT may be of special value for measuring the thickness of optically anisotropic surface layers, elucidation of mechanisms underlying planar and homeotropic orientation of molecular chains with respect to the film surface, investigations into the kinetics of orientational order formation, the role of the support in this process, and the effect of the chemical structure of molecular networks on the properties of surface layers.

The present review summarizes the most important data on the structure and optical anisotropy of polymer surface layers and the kinetics of their formation.

2. Theoretical and methodological basis of surface birefringence studies

2.1 The theory of surface birefringence in polymer films

Let the film surface (x, y) be oriented vertically (y is the vertical axis) and the incident beam lie at the horizontal plane (x, z) and be polarized at an angle of $\pi/4$ relative to the normal (Fig. 1). Then, the difference between polarizabilities of anisotropic elements in the chain $\Delta_{\gamma\vartheta}$ along the vertical and horizontal axes at the plane normal to the incident beam will cause birefringence. The above polarizability difference is a function of the polar (ϑ) and azimuthal (γ) angles of the orientation of chain elements measured from axes z and x respectively. It is easy to demonstrate that the expression for $\Delta_{\gamma\vartheta}$ will have the form [9, 15]

$$\Delta_{\gamma\vartheta} = (a_{\parallel} - a_{\perp})\left[\sin^2\vartheta(\sin^2\gamma + \sin^2\beta - \cos^2\gamma\cos^2\beta) - \sin^2\beta\right], \quad (1)$$

where $a_{\parallel} - a_{\perp}$ is the difference between the main polarizabilities of an anisotropic element of the chain and β is the angle of incidence of plane-polarized light onto the film. It is natural to choose a monomer unit as the anisotropic element.

The specific polarizability P_H can be found by integrating expression (1) over angles γ and ϑ and reducing the result to the unit volume, on the assumption that the angular distributions of monomer orientations at γ and ϑ are independent. The angular distribution at γ will be uniform [the probability density $f(\gamma) = \pi/2$)] because the film does not exhibit optical anisotropy at the normal incidence of the beam ($\beta = 0$):

$$P_H = -N_0(a_{\parallel} - a_{\perp})\sin^2\beta\int_0^{\pi}\frac{1}{2}(3\cos^2\vartheta - 1)f_H(\vartheta)\,\mathrm{d}\vartheta\,, \quad (2)$$

where N_0 is the number of monomers in the unit volume, P_H and $f_H(\vartheta)$ are the polarizability and distribution density at ϑ in the layer $\mathrm{d}H$ respectively.

Utilizing the Lorentz–Lorenz relation, it is possible to determine the phase difference δ:

$$\delta = -\frac{2\pi}{\lambda\bar{n}}\left(\frac{\bar{n}^2+2}{3}\right)^2 N_0(a_{\parallel} - a_{\perp})\sin^2\beta \times \int_0^{\pi}\int_0^{H}\frac{1}{2}(3\cos^2\vartheta - 1)f_H(\vartheta)\,\mathrm{d}\vartheta\,\mathrm{d}H\,, \quad (3)$$

where $\bar{n}$ is the mean refractive index of the polymer, H is the film thickness, and λ is the incident light wavelength.

Substituting the transmittance angle β by the incidence angle i and using the expression

$$S = \frac{1}{2}(3\overline{\cos^2\vartheta} - 1) = \frac{1}{H}\int_0^{\pi}\int_0^{H}\frac{1}{2}(3\cos^2\vartheta - 1)f_H(\vartheta)\,\mathrm{d}\vartheta\,\mathrm{d}H \quad (4)$$

for the orientational order parameter S, it is possible to write expression (3) in the following form:

$$\delta = -\frac{\pi}{\lambda\bar{n}^3}\left(\frac{\bar{n}^2+2}{3}\right)^2 N_0(a_{\parallel} - a_{\perp})SH(1 - \cos 2i)\,. \quad (5)$$

Formula (5) is the general expression for the dependence of birefringence on the incidence angle relative to the film surface.

When molecular chains have no predominant orientation ($\overline{\cos^2\vartheta} = 1/3$, $S = 0$), the film remains isotropic at any incidence angle. If the film consists of ordered molecular chains ($S \neq 0$), it will seem optically isotropic as the beam passes through it perpendicularly to the surface. As soon as the beam deviates from the normal, it undergoes birefringence with a phase difference

$$\delta = B(1 - \cos 2i)\,. \quad (6)$$

The coefficient of proportionality,

$$B = -\frac{\pi N_0 H(a_{\parallel} - a_{\perp})}{\bar{n}^3\lambda}\left(\frac{\bar{n}^2+2}{3}\right)^2 S\,, \quad (7)$$

is equal to the phase difference and, arising in the film as the beam passes through it at the angle of $\pi/4$ to the surface, it depends on both the optical properties of molecular chains and their orientational order.

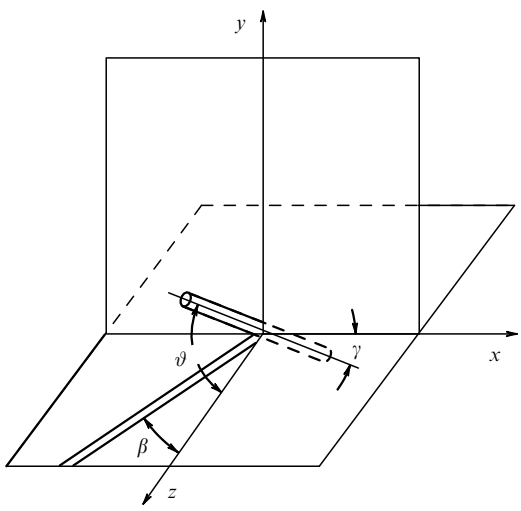

Figure 1. Geometry of a beam passing through a polymer film (see text for explanation).

2.2 Types of orientational order in surface layers

The order parameter $S_{\alpha\beta}$ may serve as the quantitative measure of orientational order of structural elements in a chain molecule with respect to the film surface. In the general case, this parameter can be expressed as the symmetric diagonal order tensor. Elements of $S_{\alpha\beta}$ are time-averaged values of the direction cosines l_{α} relating the axes of a molecule (x, y, z) to a selected axis (in our case, the normal to the film surface).

Elements of the order tensor can be expressed in the following form [17–19]:

$$S_{\alpha\beta} = \left\langle \frac{1}{2}(l_\alpha l_\beta - \delta_{\alpha\beta}) \right\rangle . \tag{8}$$

Here, $\delta_{\alpha\beta}$ is the Kronecker delta, and $\alpha\beta = x, y, z$. For axially symmetric molecules, the number of tensor elements is reduced to one

$$S_{zz} = \left\langle \frac{1}{2}(3\cos^2\vartheta - 1) \right\rangle . \tag{9}$$

In the absence of birefringence in the polymer film surface onto which a beam of light falls normally, ordering of molecular chains in the surface layers must obey the condition of uniform distribution of chain fragments at an azimuthal angle γ (see Fig. 1). Two types of ordering in surface layers meet this condition (Fig. 2). One is planar ordering which leads to the predominant disposition of chain elements parallel to the film surface (Fig. 2a). The other is normal ordering at which molecular chains are on the whole arranged perpendicular to the film surface (Fig. 2b). In both cases, the film behaves as if optically isotropic when the beam falls normally but shows birefringence in proportion to the variable $1 - \cos 2i$ when the beam deviates from the normal. However, the resulting birefringence is of the opposite sign which allows the type of ordering in the surface layers to be identified. Evidently, when chains are oriented parallel to the film surface, i.e. when $123° > \bar{\vartheta} > 57°$, then the orientational order parameter (9) $S < 0$ ($S = -1/2$ in the case of complete planar ordering). When the chains are arranged normally to the surface ($57° > \bar{\vartheta} > -57°$), the orientational order parameter $S > 0$ and becomes unity after complete normal ordering is achieved.

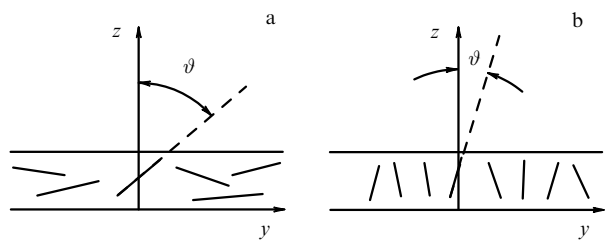

Figure 2. Possible types of ordering in surface layers of polymer films responsible for birefringence: (a) planar ordering), (b) normal ordering.

2.3 Some aspects of the experimental technique

Birefringence is measured with standard instruments for visual or photoelectric recording of the optical phase difference [20, 21]. Figure 3 schematically represents one such measuring device. The film being examined is fixed at the turn-table with the vertical axis parallel to the film surface. The film is placed between two crossed polarizing prisms P and A (P is the polarizer, A is the analyzer). The plane of polarization lies at an angle of 45° to the vertical line. The condenser O_1 focuses the bulb's filament on the film, and the thin lens O_2 projects the filament's image on the half-tone plate, a part of the Breis compensator (K). The eyepiece is focused on the half-tone. The Breis compensator consists of a thin mica plate attached to the limb and a thin half-tone plate which covers half of the field of vision. The compensator is usually $0.01-0.1\ \lambda$ thick, depending on the expected birefringence value. The optical phase difference δ in the polymer film is created by limb rotation, setting the compensator so as to have the two halves of the field of vision equally illuminated (half-tone azimuth). When the phase difference δ_0 created by the compensator is small, it is possible to write

$$\delta = \delta_0 \sin 2\Delta\varphi , \tag{10}$$

where $\Delta\varphi = \varphi - \varphi_0$ is the difference between readings of the compensator when the film is positioned at an angle to the optical axis and the polarized light falls normally to its surface.

This technique is used to study polymer films of different chemical composition prepared by evaporating solutions on various types of supports. Sometimes polymer networks are synthesized in a gap between two parallel plates of glass or other materials.

Figure 4a shows typical plots of phase difference δ vs angle i of light incidence onto the film surface for certain polymers.

In order to obtain the surface birefringence coefficients, these dependences should be presented as straight lines by plotting δ values from $1 - \cos 2i$. According to formula (6), the slopes of such straight lines may serve to determine both the degree and the sign of surface birefringence. Table 1 presents coefficients B derived from the slopes of straight lines in Fig. 4b.

3. Optical anisotropy and structural patterns of surface layers

3.1 Orientational order in surface layers of amorphous polymers

It follows from formula (7) that in the case of planar orientational order the sign of B must coincide with that for

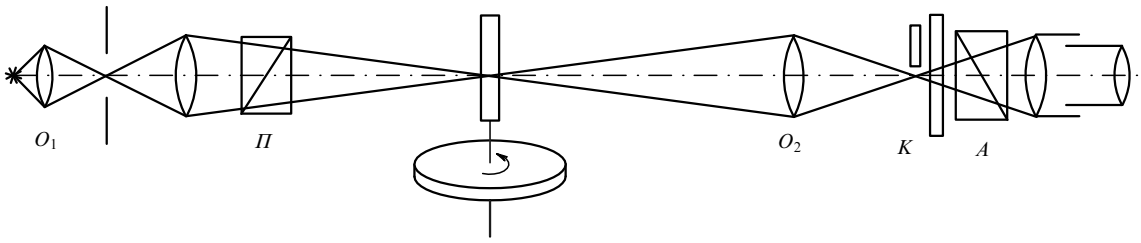

Figure 3. Schematic of the experimental arrangement for birefringence studies (see text for details).

Table 1. Principal characteristics of polymers included in the study.

Sample	Polymer†	$B \times 10^2$	$(a_{\parallel} - a_{\perp}) \times 10^{31}$, m^3	M $\times 10^{-4}$, g mol^{-1}	$A \times 10^{10}$, m	$H_0 \times 10^7$, m
1.	Polystyrene	−2.1	−18	175	20	12
2.	Polymetacrylate	−0.15	−1.4	20	15	9
3.	Cyclolinear polyphenyl sesquioxane	−21	−26	50	140	200
4.	Poly-alpha-methyl styrene	−7.8	−20	50	23	44
5.	Ethylcellulose (2.5)	6.6	20	4	200	70
6.	Cellulose monophenylacetate (2.0)	6.6	9	33	260	170
7.	Cellulose diphenylacetate (1.5)	9.9	40	22	180	90
8.	Cellulose phenylcarbamate (2.3)	−7.4	−26	15	210	120
9.	Polycyclohexymetacrylate	−0.05	5	—	—	—
10.	Cellulose acetate (2.5)	1.8	—	70	—	—
11.	Cellulose acetobutyrate (2.3)	2.7	—	4	—	—
12.	Polyimide	55	160	—	20	200
13.	Glass	0	—	—	—	—

† The level of substitution is shown in brackets.

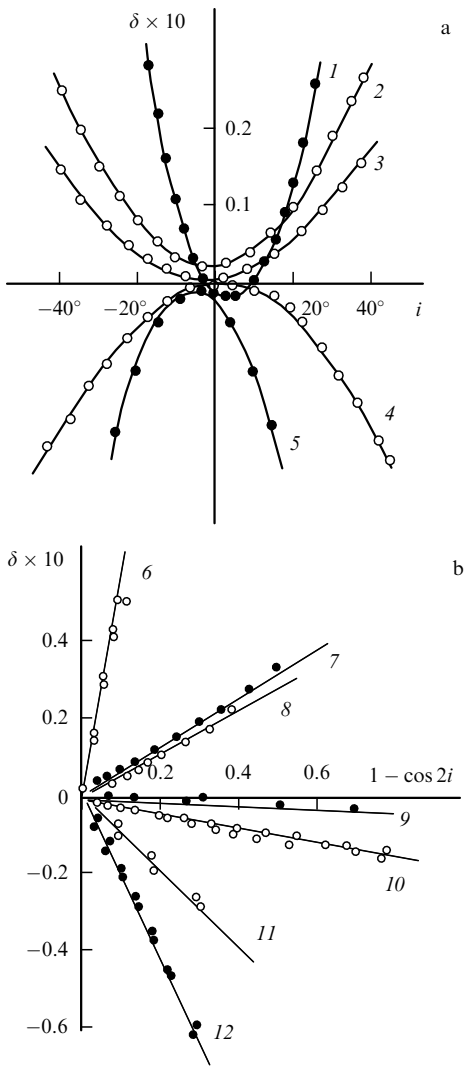

Figure 4. Plots of birefringence δ vs incidence angles i (a) and $1 - \cos 2i$ (b): *1* — cellulose diphenylacetate (CDPA); *2* — cellulose acetobutyrate (CACB); *3* — cellulose acetate (CA); *4* — PS; *5* — cellulose phenylcarbamate (CPC); *6* — polyimide (PI); *7* — ethylcellulose (EC); *8* — cellulose monophenylacetate (CMPA); *9* — polycyclohexymetacrylate (PCHMA); *10* — PMMA; *11* — poly-alpha-methyl styrene (PAMS); *12* — cyclolinear polyphenyl sesquioxane (CLPS).

anisotropy of polarizability $a_{\parallel} - a_{\perp}$ of a structural element in the chain molecule; in the case of normal ordering, B and $a_{\parallel} - a_{\perp}$ must have opposite signs.

It can be inferred from the comparison of coefficients B in Table 1 and the $a_{\parallel} - a_{\perp}$ values that films of amorphous polymers listed in the table exhibit planar ordering of molecular chains characteristic of cholesteric liquid crystals.

It should be borne in mind that the $a_{\parallel} - a_{\perp}$ values shown in the table are based on measurements of segmental anisotropy $\alpha_1 - \alpha_2$ in solutions and may have different signs compared with analogous values obtained in the studies of corresponding block-polymers [20–22]. This is actually the case at small absolute values of $a_{\parallel} - a_{\perp}$. For example, curve *10* in Fig. 4b shows the dependence of δ on $1 - \cos 2i$ for a sample of atactic polymethyl metacrylate (PMMA). Clearly, the PMMA film shows negative surface birefringence. That is, it has the same sign as segmental anisotropy measured in a block near the glass transition temperature [22], in contrast to positive segmental anisotropy in the solution [21]. The same may be true of a sample of polycetylhexyl metacrylate (PCHMA) (curve *9* in Fig. 4b).

3.2 Orientational order distribution across the film thickness

An important issue in the study of spontaneous orientation of molecular chains in polymer films is the location of the ordered layer, because ordering may be either confined to the surface layer or uniformly distributed across the film. The problem can be solved by examining a set of films of different thicknesses. Figure 5 shows that double refraction does not significantly depend on the film thickness provided it is sufficiently large. This indicates that the orientation order of molecular chains is an intrinsic feature of surface layers. In very thin films, birefringence decreases with decreasing thickness.

It is possible to obtain the distribution of molecular chain ordering across a polymer film from the H-dependence of coefficient B (see Fig. 5). Differentiating expression (7) with respect to H and using formula (4) yields

$$S(H) = \frac{\mathrm{d}}{\mathrm{d}H}\int_0^H S_H \,\mathrm{d}H = -\left(\frac{3}{\bar{n}^2 + 2}\right)^2 \frac{\bar{n}^3 \lambda}{N_0 (a_{\parallel} - a_{\perp})} \frac{\mathrm{d}B}{\mathrm{d}H} . \tag{11}$$

It follows from formula (11) that the dependence of the ordering factor on the film thickness coincides with the derivative of the H-dependence of B to within the constant

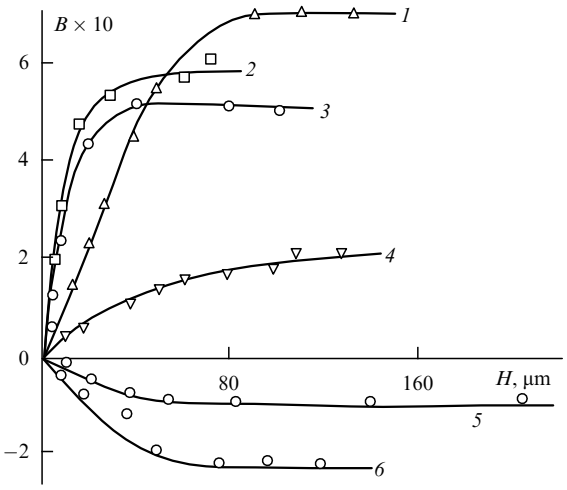

Figure 5. Plots of birefringence B vs polymer film thickness H: *1* — cellulose acetate; *2* — polyamidoimide; *3* — polyimide; *4* — cellulose acetate film formed at the mercury surface (axis of ordinates scale is 10 times that of the axis of abscissas); *5* — polystyrene (scale 5 : 1); *6* — CLPS.

multiplier. Figure 6 shows the ordering factor distribution in PI, PS, CLPS, and polyamidoimide films. It can be seen that ordering in polymer films is characterized by negative values of the parameter S and is manifest at a distance of 10^2 μm from the surface adjacent to the support. This observation is illustrated by Fig. 7 showing a microphotograph of a thin section through a cellulose acetate film taken in crossed nicols. The thickness of the oriented (lucid) layer at the lower surface is around 100 μm, in good agreement with curve *1* in Fig. 5 (the $B(H)$ curve for the CA film is saturated at $H \approx 80$ μm).

A notable finding is the very high degree of ordering in PI films (curve *3* in Fig. 6) which suggests almost complete planar orientation of molecules in the surface layers of this polymer.

3.3 The equivalent surface layer

The distribution of orientational order across a polymer film is evaluated from birefringence measurements in a set of polymer films of different thicknesses, using Eqn (11). This

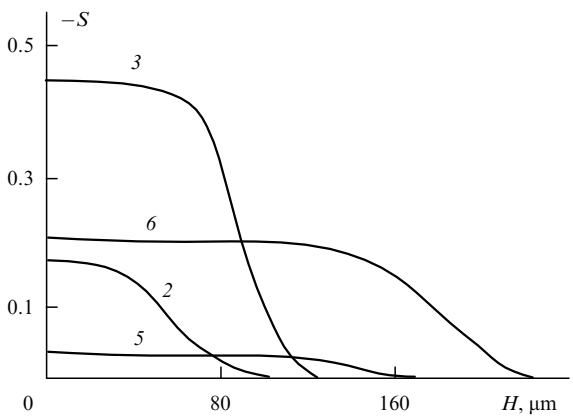

Figure 6. The distribution of orientational order across polymer films (see Fig. 5 for notation).

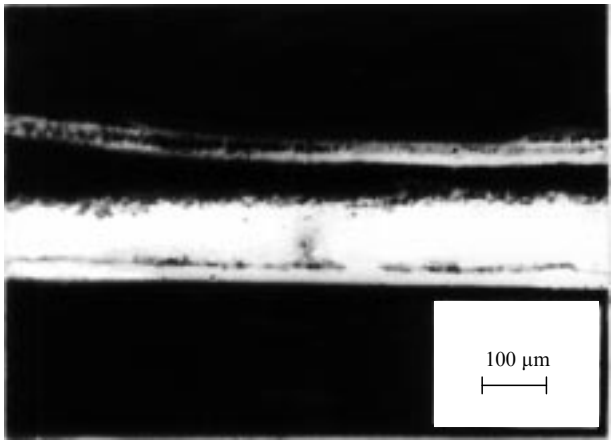

Figure 7. Micrograph of a thin section through cellulose acetate film in crossed nicols.

approach is rather laborious which accounts for the introduction of the equivalent surface layer concept to facilitate the assessment of orientational order in polymers.

Let us assume that planar ordering of chain molecules in the surface layer of a polymer extends to a depth H_0 but disappears in deeper layers. The thickness of such an equivalent layer can be found by substituting the order parameter $S = -0.5$, corresponding to complete planar ordering, into formula (7):

$$H_0 = \frac{2B\bar{n}^3\lambda}{N_0\pi(a_{\parallel} - a_{\perp})}\left(\frac{3}{\bar{n}^2 + 2}\right)^2 . \qquad (12)$$

H_0 values calculated using formula (12) are listed in Table 1.

It should be borne in mind that these H_0 values represent the minimal thickness of anisotropic surface layers since molecular chain ordering in real polymer films is never complete (see Fig. 6). Nevertheless, the H_0 values in Table 1 are very large giving evidence of the parallel arrangement of tens of thousands of molecular chains.

Let us now discuss possible mechanisms of planar ordering. In the first place, the planar arrangement of molecular chains in polymer films appears to be governed by the support. Their orientation may result from steric effects. In other words, segments of macromolecules absorbed by the surface have planar orientation which decreases due to chain elasticity. Obviously, the thickness of the ordered layer must be commensurable with the length of segment A.

However, comparison between computed H_0 values in Table 1 and segment lengths shows that they are 3 – 4 orders of magnitude higher than A lengths.

An alternative explanation of planar ordering is based on the assumption that polymer molecules interact with the solid surface and this interaction affects deeper layers of the polymer solution, being responsible for polymer chain orientation in the course of film formation. Certain authors [23 – 25] suggest that such interactions take place during adsorption of polymer molecules onto solid surfaces of the support. However, observations of polymer solutions through which a beam of light passes at an angle failed to reveal marked birefrigence and thus macroscopically apparent polymer adsorption on the support (see Section 6.2, Figs 22 and 23).

Kargin, Kozlov et al. [26, 27] hypothesized that planar ordering in polymer films is a result of the mechanical stress which develops in a gel upon removal of the solvent.

Indeed, the process of film formation in the general case is described by the Maxwell equation

$$\frac{\mathrm{d}\sigma}{\mathrm{d}t} = E(c)\frac{\mathrm{d}\varepsilon}{\mathrm{d}t} - \frac{\sigma}{\tau_0(c)}\,,$$

where σ is the stress, ε is the resulting strain, $\tau_0(c)$ is the relaxation time, and $E(c)$ is the Young modulus.

Concentration-related variations of the Young modulus and relaxation time depend on the viscosity of polymer solutions. At the gel-formation point ($\tau_0 \to \infty$),

$$\frac{\mathrm{d}\sigma}{\mathrm{d}t} = E\,\frac{\mathrm{d}\varepsilon}{\mathrm{d}t}\,, \qquad \sigma = E\Delta V^{\beta}\,,$$

where ΔV is the change of volume and β is the constant which characterizes high elasticity of the polymer gel.

In other words, stress evolves in the film as its volume changes while the polymer adheres to the support during evaporation of the solution.

The authors maintain that polymer orientation can be hypothetically described as a two-stage process, i.e. isotropic shrinkage of the solution to a film of a finite volume followed by its biaxial extension to the equivalent of the lining area.

3.4 Effect of supports on the surface optical properties of polyparaxylylene

Thin films of polyparaxylylene (PPX) were obtained by polymerization from the gaseous phase of diparaxylylene used as the raw substance. Polymerization was realized on steel or glass supports [28].

In accordance with the birefringence theory, the value B (7) turned out to be proportional to the film thickness H at smaller H values. The H-dependence of B is represented in Fig. 8. It is clear that the thickness of the optically anisotropic PPX layer is not less than 10 μm.

In order to characterize the orientational order, it is necessary to evaluate the optical anisotropy $\Delta a = a_{\parallel} - a_{\perp}$ of a PPX monomer unit.

For the calculation of Δa, it is convenient to begin by estimating the difference between the main polarizabilities

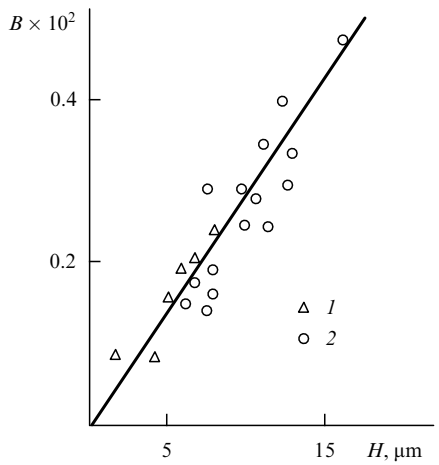

Figure 8. Birefringence B of polyparaxylylene (PPX) vs film thickness H on glass (*1*) and steel (*2*) supports.

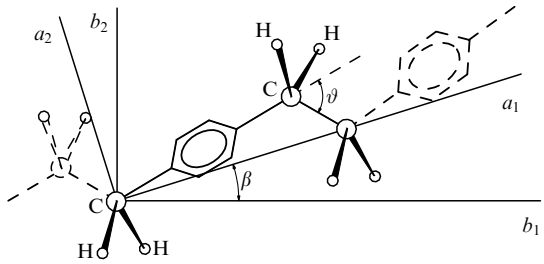

Figure 9. Explanatory scheme for the calculation of optical anisotropy of PPX monomer unit.

Δb of a PPX monomer unit with respect to axes (b_1, b_2) because in these axes C–C bonds are oriented at the same angle $\varphi_1 = \vartheta/2$ to axis b_1 and all C–H bonds are positioned at the same angle $\varphi_2 = \pi/2$ (Fig. 9). The value of Δb can be found from the formula

$$\Delta b = \Delta b^{\mathrm{Ph}} + 3\Delta b^{\mathrm{C-C}}\,F(\varphi_1) + 4\Delta b^{\mathrm{C-H}}\,F(\varphi_2)\,. \qquad (13)$$

Here, Δb^{Ph} is the optical anisotropy of the phenyl radical, $\Delta b^{\mathrm{C-C}}$ and $\Delta b^{\mathrm{C-H}}$ are the optical anisotropies of C–C and C–H bonds, and $F(\varphi_i)$ is the orientation function of C–C and C–H bonds with respect to the axis (a_1, a_2).

In the molecular axes (a_1, a_2), the optical anisotropy of the PPX momomer unit is obtained from the formula

$$\Delta a = \frac{1}{2}\,\Delta b(3\cos^2\beta - 1)\,. \qquad (14)$$

The physical sense of the angle β is apparent from Fig. 9. Thus, $\Delta a = +50 \times 10^{-31}$ m^3.

Since $\Delta a > 0$ and $B > 0$, the orientational order parameter $S < 0$, in accordance with formula (7). Hence, the angle between the segment's axis and the normal to the film surface lies in the range $123^\circ > \vartheta > 57^\circ$. In other words, molecular chains of PPX in the surface layers of thin films are largely oriented parallel to the film surface.

It is worthy of note that the H-dependences of B for films on steel and glass supports practically coincide. This means that the properties of the support are of no great consequence for the surface anisotropy of adhesive PPX films.

4. Properties and structure of surface layers in epoxypolymer networks

4.1 Thickness and orientation of surface layers

Let us consider the results of investigations into surface anisotropy of tightly cross-linked polymer networks using epoxide compositions as a model [10, 29].

Films of epoxyresins were prepared by hardening resorcine diglycidyl ether (RDGE),

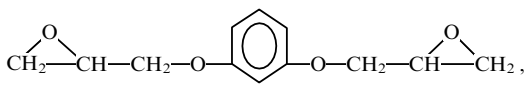

diethyleneglycole diglycidyl ether (DEG),

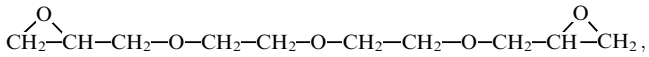

and diphenylopropane diglycidyl ether (DPDE)

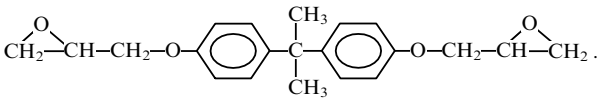

The hardening agents were metaphenylene diamine (m-PDA) and 1.5-diaminopentene (DAP):

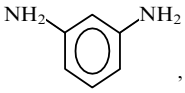

, $NH_2—(CH_2)_5—NH_2$.

The chemical structure of the components of these polymers is presented in Table 2. Hardening occurred between two glass plates. The film thickness depended on the gap width.

Table 2. Characteristics of epoxypolymer networks.

Sample	Copolymer components	Functional group ratio
1.	RDGE, PDA	1.0 : 1.0
2.	DEG, PDA	1.0 : 1.0
3.	RDGE, DAP	1.0 : 1.0
4.	DEG, RDGE, PDA	0.3 : 0.7 : 1.0
5.	DEG, RDGE, PDA	0.7 : 0.3 : 1.0
6.	DPDE, PDA	1.0 : 1.0

Let us consider a three-layer structure as a thin film model. Two layers of thickness H_x adhere to the film surfaces and their structural elements are organized with respect to these surfaces. The third layer having a thickness H_a is enclosed between the two others and its molecular chains consist of isotropically oriented elements.

Evidently, the contribution of the anisotropic surface layers to birefringence is proportional to the film thickness $H < 2H_x$. This was experimentally confirmed for samples 1, 3, 4, and 6 (Fig. 10).

It may be expected that B values for films having a thickness $H > 2H_x$ will be independent of H. Indeed, this proved to be true of sample 6 (see Fig. 10). The model being considered allows the thickness of an optically anisotropic surface layer to be measured.

Figure 10 shows that the surface layer in sample 1 is more than 0.2 mm thick; it is $H_x > 0.23$ mm in sample 3, $H_x \approx 0.3$ mm in sample 4, and $H_x \approx 0.6$ mm in sample 6.

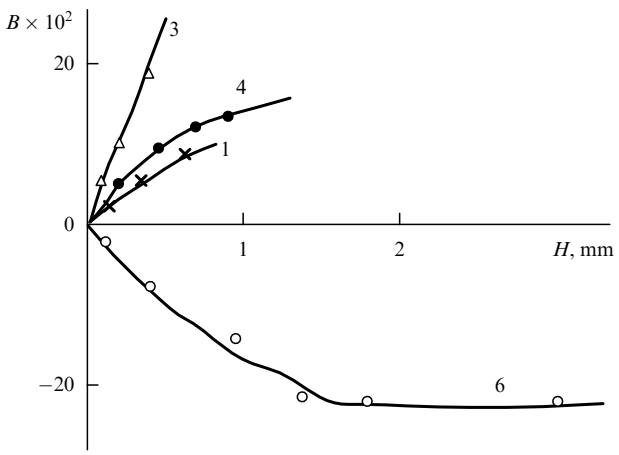

Figure 10. B plotted against H. The figures correspond to the sample numbers in Table 2.

The estimated thickness of surface layers in epoxyresin films is 10 times that in other polymers (see Table 1).

There is a significant correlation between the above estimates of the thickness of anisotropic surface layers and their enhanced density (for a given volume) conditioned by the diffusion mechanism of volume relaxation [12].

The orientation of molecular chains in polymer networks was deduced from the temperature-dependence of the photoelasticity coefficient $\varepsilon = f(T)$ for the polymers included in the study [29]. These dependences were used to determine ε values in highly elastic states of these polymers. For sample 6, $\varepsilon = +2.0 \times 10^{-9}$ Pa^{-1}.

Also, the knowledge of ε proved useful in the assessment of the optical anisotropy of a statistical segment $\alpha_1 - \alpha_2$ in branches of the molecular network, based on the Coon–Treolar formula

$$\varepsilon = \frac{2\pi}{45kT}\frac{(n^2+2)^2}{n}(\alpha_1 - \alpha_2)\,. \tag{15}$$

It was found that $\alpha_1 - \alpha_2 = +84 \times 10^{-31}$ m^3.

These results help to characterize the orientation of the branches of the examined networks relative to the film surface.

Experimentally found values of B and $\alpha_1 - \alpha_2$ for samples 2, 3, and 4 are positive. Therefore, $S < 0$, in accordance with formula (7). This means that molecular fragments in the surface layer of the examined networks are largely arranged parallel to the film surface. Unexpected results were obtained in a study of sample 6. It follows from $\alpha_1 - \alpha_2 > 0$ and $B < 0$ that molecular chains in this network should be oriented normally to the film surface. Sample 6 was prepared using metaphenylene diamine (m-PDA) as the cross-linking agent with a large dipole moment. In order to elucidate the possible role of the dipole moment in the unusual orientation of the branches with respect to the film surface, we synthesized a molecular network using paraphenyldiamine (p-PDA) as the cross-linking agent.

Figure 11 shows δ vs i curves for DPDE cross-linked with p-PDA (curve *1*: $H = 0.19 \times 10^{-3}$ m and curve *2*: $H = 0.37 \times 10^{-3}$ m) or m-PDA (curve *3*). It can be seen that the sign of δ is negative when m-PDA is used to achieve cross-linking of the epoxyresin and positive when the resin is cross-linked with p-PDA. It follows that in the former system interjunction chains are largely oriented normally to the film surface whereas in the latter they are parallel to it. This

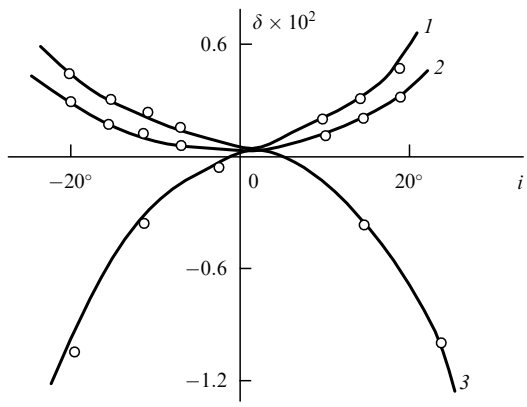

Figure 11. δ vs i for DPDE cross-linked with p-PDA (curves *1* — $H = 0.19 \times 10^{-3}$ m, *2* — $H = 0.37 \times 10^{-3}$ m) and mPDA (curve *3*).

paradoxical finding remains to be explained. It is tentatively conjectured that the geometry of junctions is of importance for chain packing in the denser surface layer of the network. The m-PDA molecule has large dipole moment which is lacking in p-PDA.

4.2 The role of kinetic effects in the formation of surface anisotropy

Cross-linked polymer systems (molecular networks) are useful models for a study of temperature-dependent physical properties because the samples retain their shape as the temperature rises to the thermal disintegration point. This explains why we used the polymer compositions described in the previous Section [29] to examine kinetic effects.

Studies using angular BT have demonstrated that the optical anisotropy of surface layers disappears if the samples are subject to sequential annealing and quenching, i.e. heating in excess of the glass transition temperature T_c followed by rapid cooling. Moreover, it has been shown [29] that polymers in the highly elastic state exhibit no surface optical anisotropy. This is natural because thermal motion of chain molecules and their fragments lead to disorientation and the resulting disorder is 'frozen' after quenching. It appears that anisotropic properties of surface layers are formed in the vicinity of the glassing point. This hypothesis was verified in a study of the film (sample 6) cast at $T = T_c + 5\,^\circ\mathrm{C}$.

Figure 12 shows plots of δ versus $1 - \cos 2i$ for films of similar thickness (sample 6) that underwent annealing for different time periods. It can be seen that surface optical anisotropy grows with increasing annealing time.

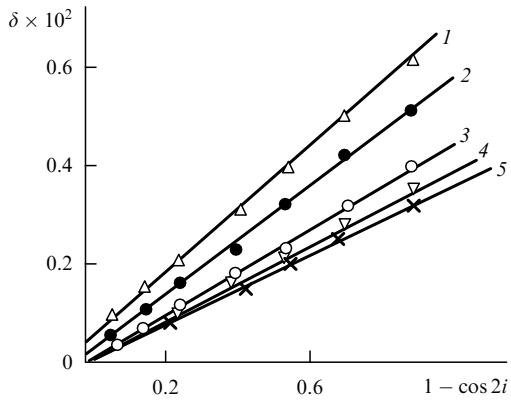

Figure 12. Variation of δ with $1 - \cos 2i$ for films of sample 6 (Table 2): $H = 75\,\mu\mathrm{m}$ (*1*), 90 (*2*), 100 (*3* and *5*), and 80 (*4*); hardening for $t = 30$ (*1*), 24 (*2*), 12 (*3*), 6 (*4*), and 0 hrs (*5*).

Figure 13 shows the dependence of B/H on the annealing time t. Optical anisotropy increases with the duration of annealing. This finding is of primary importance for the elucidation of the orientational order mechanism in surface layers.

The effect of the support in the above experiment was excluded by placing the films in air.

The experiments presented in Figs 12 and 13 provided unambiguous evidence of the important role of kinetic effects in the creation of the gradient of surface physical properties in polymer materials.

In the following section, we shall again discuss mechanisms of orientational order in surface layers of thermally treated polymer films.

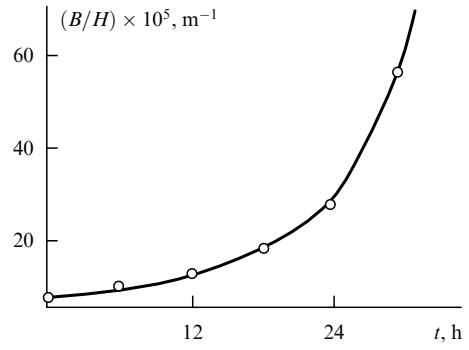

Figure 13. B/H as a function of annealing time t for sample 6 (Table 2).

5. Formation of surface layers in block-copolymers

5.1 Surface optical properties of polyether-based ureourethane

Synthesis of block-copolymers is a promising tool for polymer modification and the development of polymer materials with novel properties. Of special interest is the opportunity to control the structure and properties of block-copolymers containing thermodynamically flexible and rigid blocks [30 – 32].

Most of the specific properties intrinsic in such block-copolymers are due to their two-phase morphology in which one component is represented by domains distributed in the matrix of the other [33 – 39]. When the concentration of domains formed by rigid blocks is low, the mechanical properties of the system are in fact those of the matrix. As the concentration of the rigid blocks grows, the domains assemble in clusters and can even give rise to a percolation cluster.

The structure of surface layers in such polymer systems is of great interest [33]. However, data on the orientational order of molecular chains and structural features of surface layers are lacking from the literature despite numerous studies devoted to polymer materials.

Refs [34, 35] report interesting data on the molecular and supramolecular structure and surface properties of segmented polyether-based ureourethanes (PEBUU) composed of a sequence of alternating flexible and rigid blocks.

The chemical formula of these PEBUU has the general form

$$-\left[\mathrm{C(O)NHR'NHC(O)NHRNHC(O)NH}\right]_n- \\ -\left[\mathrm{R'NHC(O)OR''O}\right]_m-\,,$$

where R is the oligourethane diamine (BD-3) residue $-\mathrm{R'NHC(O)OR'''OC(O)NHR'}-$; R′ is the 4,4′-diphenylmethane diisocyanite (MDI) residue $-\mathrm{C_6H_4CH_2C_6H_4}-$; R″ is the polyfurite (PF) residue $-\left[(\mathrm{CH_2})_4\mathrm{O}\right]_{14}(\mathrm{CH_2})_4-$; R‴ is the tetrabutanediol residue $-\left[(\mathrm{CH_2})_4\mathrm{O}\right]_3(\mathrm{CH_2})_4-$.

The polymers were synthesized in the reaction of MDI with a mixture of oligourethane diamine and PF in a 10% DMPA solution. The 0.1 mole difference in the hydroxyl to amine ratio BD-3/PF between consecutive samples is reflected in their numbering:

$$1 \to 1.0/0.0\,,\quad 2 \to 0.9/0.1\,,\ldots,10 \to 0.1/0.9\,.$$

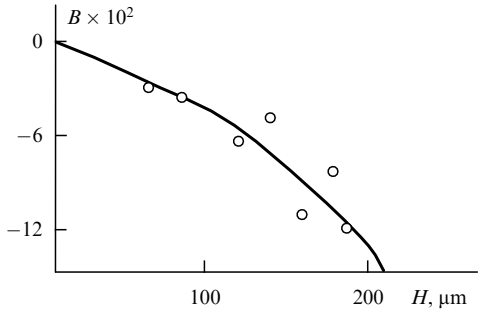

Figure 14. B as a function of H for PEBUU films.

The concentration of rigid blocks containing phenyl nuclei is expressed through blocks $[n]$ and $[m]$ content, i.e. as the relative molar concentration of corresponding blocks $K = [n]/([n] + [m])$.

The relationship between birefringence and the angle i at which the light beam falls onto a film was studied in Ref. [35]. Figure 14 shows the dependence of B on the thickness of PEBUU films (sample 5). The absolute value of B increases with growing H and shows no tendency to saturation until $H \approx 200$ μm. This allows the thickness of the optically anisotropic surface layer to be determined. Based on the three-layer model of polymer films, it is inferred that $H > 100$ μm.

When polarized light falls onto the film at an angle, it undergoes birefringence with negative sign. Given experimental values of $B < 0$ and $\alpha_1 - \alpha_2 > 0$ [38], the order parameter $S > 0$; hence, the mean angle between the molecular chains of PEBUU and the normal to the film surface is $\vartheta < 57°$. In other words, fragments of molecular chains in the surface layers of PEBUU samples are largely oriented perpendicular to the film surface.

This can be explained in terms of a molecular model (Fig. 15) in which rigid PEBUU blocks made domains embedded in a matrix of flexible PF chains [34, 35, 38]. It is supposed that supramolecular structures (domains) in surface layers are largely oriented parallel to the film surface. At the same time, molecular fragments (rigid blocks) in the domains are on the whole arranged perpendicular to the axes of maximum domain stretching [38]. Hence, on the average molecular chains are oriented perpendicular to the film surface (Fig. 15).

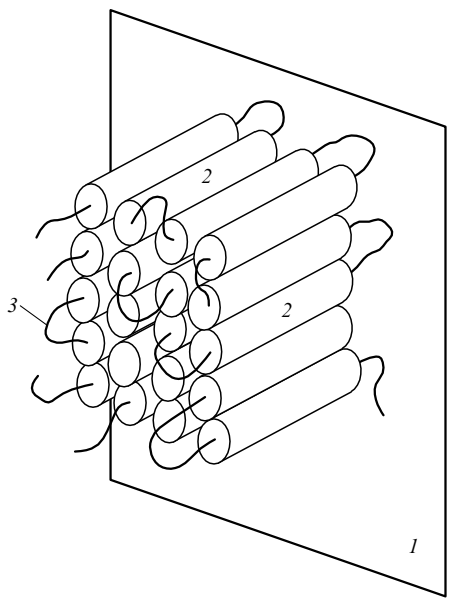

Figure 15. A model showing domain orientation in PEBUU surface layers: *1* — film surface, *2* — rigid blocks, *3* — flexible blocks.

Ref. [35] also considered the temperature-dependence of birefringence for polarized light transmitted through the film at an angle. Fig. 16 shows plots of $\Delta\varphi$ versus T ($\Delta\varphi$ being proportional to the birefringence) for samples 2, 4, 5, and 6 at a fixed incidence angle ($i = 15°$). It can be seen that absolute $\Delta\varphi$ values grow spontaneously with T in the temperature range 100 to 140 °C. This means additional domain ordering with respect to the film surface in the 100 – 140 °C range which corresponds to the autonomous mobility of supramolecular structures (domains) at $T = 130$ °C [34, 38]. Surface tension forces acting on anisodiametrical domains cause their additional spontaneous orientation relative to the film surface.

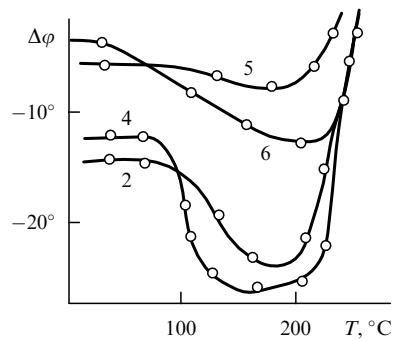

Figure 16. Temperature-dependence of $\Delta\varphi$. Figures correspond to sample numbers in Table 2.

Taken together, these results indicate that the orientation process in surface layers involves not only molecular fragments but also anisodiametrical supramolecular structures, if conditions permit [9, 10, 29]. This again emphasizes the important role of kinetic effects in the creation of the gradient of physical properties near the surface of polymer materials.

At $T = 200 - 280$ °C, domain 'melting' occurs, and the polymer undergoes a transition to the isotropic, highly elastic state. Concurrently, surface layers lose anisotropic properties. The transition temperature is strongly dependent on the concentration of rigid blocks in co-polyurethane.

The relationship between the temperature of PEBUU transition to the highly elastic state and the rigid block content is illustrated by Fig. 17. This figure also shows the K-dependence of surface birefringence (B). The extreme nature of both dependences is obvious. A rise in the relative concentration K corresponds to an increased size of rigid the blocks contained in block-copolymers. It is expected that the domain size and the degree of orientational order for rigid blocks in the domains will also increase which automatically leads to higher absolute values of both the surface birefringence coefficient B and the temperature T of co-polyurethane transition to the highly elastic state.

However, the size of flexible blocks at $K > 0.6$ is so small that relatively large rigid blocks of co-polyurethane fail to assemble in perfect domains during film formation for steric reasons. This accounts for the decrease in both the tempera-

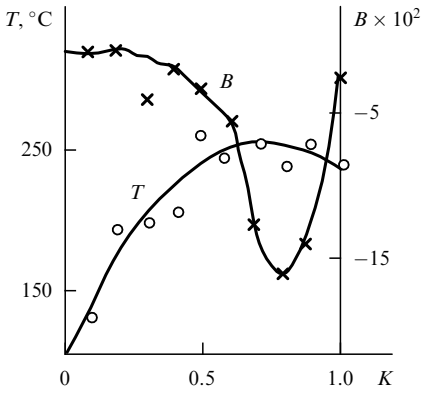

Figure 17. Influence of rigid block concentration K in copolyurethanes on B values and temperature T of PEBUU transition to the highly elastic state.

ture of transition to the highly elastic state and the surface birefringence at $K > 0.6$.

It is worthy of note that the surface birefringence coefficient B is highly sensitive to variations of $K = [n]/([n] + [m])$. Clearly, the extremum of the dependence $B = f(K)$ conforms to the morphology of block-copolyurethane with its perfect orientational order of rigid blocks in domains. This fact allows angular BT to be applied to the evaluation of maturity of supramolecular structures in polymers prone to microsegregation.

Experimentally confirmed spontaneous orientation of chain fragments and supramolecular structures relative to film surfaces prompts the conclusion that properties of polymer fibers and thin films will be essentially dependent on their thermal history which may influence the orientation of filler particles in surface layers.

The appearance of orientational order in the surface layers of thermally treated polymer films should be attributed to the effects of void volume diffusion which are responsible for a faster specific volume decrease in surface layers than in the bulk of the polymer. Diminution of the surface volume while the film area remains unaltered (in the first approximation) results in biaxial stretching of the surface layer. This process is accompanied by the predominant orientation of anisodiametrical particles (fragments of chain molecules, supramolecular structures or filler particles) parallel to the film surface which induces optical anisotropy in the surface layers.

In fact, this mechanism is physically similar to that underlying the appearance of orientational order in surface layers upon evaporation of the solvent from a gel or solution as previously described in Section 3.3. In this case, the diminished volume of surface layers and the unaltered substrate area also combine to cause biaxial stretching of the solution (or gel) in the course of drying, and hence, orientational order in surface layers.

The difference between these apparently identical mechanisms is reduced to the fact that in the former case the void volume is 'evaporated' whereas in the latter the solvent molecules are removed. In other words, the presence of interphase boundaries accounts for anisotropic transition events which lead to the appearance of regions with a conspicuous gradient of physical properties (density, orientational order, etc). As a result, surface layers of polymer films acquire properties different from those in the bulk of the polymer.

5.2 Specific surface properties of two-component copolymers

BT was employed in Ref. [40] to investigate optical anisotropy in surface layers of statistical copolymers and block-copolymers of styrene and vyniltrimethylsilane. For comparison, optical anisotropy was measured in polystyrene (PS) and polyvinyltrimethylsilane (PVTMS).

Figure 18 shows the surface birefringence coefficients B versus H (thickness) for polymer films included in the study. Evidently, PVTMS has $B > 0$ whereas PS, block-copolymer, and statistical copolymer have $B < 0$. Segmental anisotropy of polarizability for PVTMS and PS being $\alpha_1 - \alpha_2 = 62 \times 10^{-31}$ m^3 and $\alpha_1 - \alpha_2 = -179 \times 10^{-31}$ m^3 respectively [41, 42], the factor S is negative for all polymer films considered [cf. Eqn (7)]. In other words, molecular fragments in the surface layers of these polymers are largely oriented parallel to the film surface.

The use of the three-layer model of polymer films allows the thickness of surface layers to be estimated based on the analysis of the H-dependence of B (see Fig. 18). It has been shown that the thickness of PVTMS films is $H_x \approx 80$ μm and that of PS films $H_x \approx 40$ μm; for block-copolymers and statistical copolymers $H_x \approx 30$ μm. These estimates agree with the thickness measurements of surface layers in amorphous polymers reported in Section 2.

It appears from Fig. 18 that coefficient B, which characterizes surface birefringence, is positive for PVTMS and negative for PS. Naturally, it can be expected to take intermediate values for block-copolymers and statistical copolymers:

$$B = B_1(1 - x) + B_2 x\,, \tag{16}$$

where B_1 and B_2 are the surface birefringence coefficients for PVTMS and PS respectively and x is the molar styrene fraction in a given copolymer.

However, the B values for copolymers turned out to be close to the B for PS suggesting that at least one surface layer in copolymer films is enriched in molecular fragments of PS. The fact that surface properties of real block and statistical copolymers proved almost identical means that they are not directly related to microphase separation of the components. On the other hand, the similarity between copolymer and PS

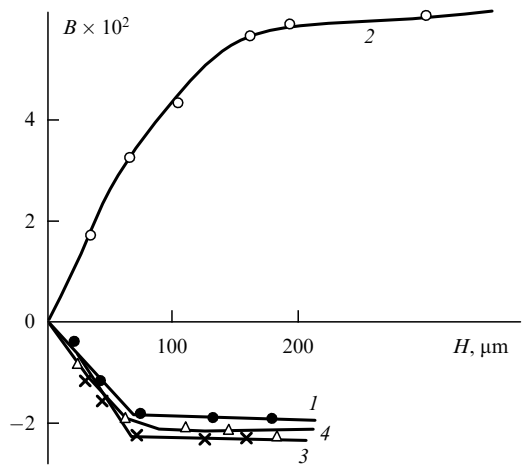

Figure 18. Plots of B vs H for polystyrene (*1*), polyvinyltrimetylsylane (*2*), statistical copolymer of styrene and vinyltrimetylsylane (*3*), PS and PVTMS block-copolymer (*4*) films.

surface properties appears to reflect a markedly inhomogeneous composition of the examined molecular structures [41].

5.3 Methods for the formation of surface layers

Investigations into properties of polymer materials in large volumes fail to provide information about their surface layers which are structurally and morphologically different from inner ones [55–61].

The difference between surface and inner layers is especially pronounced in two and multicomponent polymer systems [55, 57, 61]. For example, surface layers in polysulfone–polydimethylsiloxane (PSN–PDMS) copolymers proved to be enriched in the siloxane component [57]. Analysis of a polystyrene–polybutadiene (PS–PB) block-copolymer has demonstrated that its surface layer largely consists of polybutadiene [62] while surface layers in a polystyrene–polymethylmetacrylate (PS–PMMA) block-copolymer contain large amounts of PS [62]. These observations provide a real basis for the synthesis of polymer materials with a gradient of physical properties using multicomponent copolymers.

Ref. [63] describes the synthesis of cross-linked three-component copolymers with the desired gradient of optical properties in the surface layers. The authors managed to copolymerize styrene and ethyleneglycole dimetacrylate (EGDM) and thus obtained a two-component forepolymer matrix in the form of gel-like cylindrical specimens. At the second stage, they carried out a diffuse substitution of a part of the matrix comonomers by methylmetacrylate (MMA) with simultaneous copolymerization of the triple styrene–EGDM–MMA system. The results of this study demonstrated the possibility of the desired modification of the triple copolymer composition along the radius of a cylindrical sample to create the optimal surface gradient of optical properties for further practical application.

Specifically, this approach may be employed to develop gradient lenses to be used as light-focusing elements with a parabolic distribution of refractive index in the surface layers [63, 64].

A new type of polymer structure has recently raised considerable interest. These are gradient interpenetrating polymer networks (IPPN), i.e. polymers with a transverse concentration gradient of constituent components [61]. In a gradient IPPN of polystyrene (PS), polyacrylonitryl (PAN), and ethylene dimetacrylate (cross-linking agent), the matrix is built up of PS while PAN is located in the surface layer showing the prominent concentration gradient of this constituent along the normal to the sample surface [65].

More opportunities for the synthesis of IPPN with a gradient of physical properties in surface layers are provided by the use of thermodynamically incompatible polymers as constituent components. In such systems, segregation of incompatible units is not restricted to the formation of macroscopic phases. Instead, isolated domains of different composition evolve, each consisting of one type of unit. Local characteristics in these systems are very much unlike those averaged over the entire system's volume [59, 66]. An example of such a system is provided by gradient IPPN composed of polyethers (PE) and cross-linked polyacrylamide (PA) [61, 67]. At a certain stage, components of this system undergo microphase separation, by virtue of their thermodynamic incompatibility, and rigid blocks of PE assemble in domains which function as junction points of the molecular network. The gradient of physical properties in this system evolves for two reasons. Firstly, the network chemical composition undergoes a series of local changes as the distance from the core of the sample decreases (the surface layers of the specimen being examined are enriched in PAA). Secondly, each surface layer is a self-contained two-phase IPPN with a different phase composition. Collectively, these events are responsible for the gradient of physical properties near the IPPN surface. The resulting material contains a non-equilibrium 'frozen' structure with incomplete microphase separation. The overall properties of such systems are determined by the composition gradient, morphology, and phase ratio in different layers.

Therefore, the modification of both the properties and thickness of surface layers in gradient IPPN to produce desired materials is possible by varying the degree of thermodynamic compatibility between the matrix and the second component which penetrates it by diffusion. Also, it can be achieved by the choice of concentration of the reacting substances, the diffusion conditions, and by thermal processing to 'interrupt' the microphase separation at a desired stage.

The orientation of structural elements relative to the surface is also important for the formation of polymer surface properties [68] as illustrated by the results of experiments reported in previous sections.

Surface properties of polymer materials are responsible for their adhesiveness, friction, wetting, swelling, permeability, and biocompatibility.

The growing interest in the polymer systems described in this section is accounted for by the prospect of their extensive application in medicine, optoelectronics, instrument-making, fiber optics, etc. [55–57].

6. Orientational effects related to the formation of polymer membranes from solutions

6.1 General information

Polymer membranes are used in the separation of solutions and suspensions by reverse osmosis technology, and ultra- and micro-filtration [43, 44]. Such membranes are polymer films having thicknesses up to 100–500 μm and pores of several angstroms (reverse osmosis) to a few millimeters (microfiltration) in size. Membranes obtained by wet casting from polymer solutions are most widely used for the above purposes. In this technique, a moderately concentrated polymer solution is placed on a solid surface and brought into contact with a precipitant which results in the emergence of a porous membrane. Uniformly thick membranes with so-called isotropic structure are made with the aid of soft precipitants. Hard precipitants give rise to membranes of asymmetric structure having a dense selective layer at the boundary with the precipitant and a macroporous substructure which makes up a major part of the membrane volume. Besides the selective layer, asymmetric membranes have another dense layer near the substrate surface. The mechanism of its formation is the subject of debate.

Cellulose diacetate with a 2.5–2.6 degree of substitution is most often used to produce polymer membranes due to its prominent hydrophilic nature, limited swelling in water, ready solubility in various solvents, and rather good mechanical properties. Isotropic cellulose acetate membranes extensively exploited in this country are MGA reverse osmosis

membranes, UAM ultrafiltration membranes and MFA microfiltration membranes.

To summarize, the manufacturing of polymer membranes and dense films has much in common. In both cases, the polymer solution is cast onto a solid adhesive support, and the process results in a decrease in the solution volume. It is not surprising that investigations of polymer membranes by angular BT have revealed a substantial degree of orientational order (see Section 6.2). Further studies are needed, taking into consideration that orientational order in dispersed systems is to a large extent responsible for both their filtering capacity and mechanical strength [45]. A comparative analysis of porous membranes and much better known polymer films may be of great value in this context.

6.2 The oblique incidence method in a study of membrane structure and formation kinetics

The BT for polarized light passing across membranes at an angle to the normal has demonstrated that polymer membranes, similarly to dense films, contain a strongly ordered polymeric phase [46, 47]. Moreover, the degree of ordering in cellulose acetate membranes shows a good correlation with birefringence in films of the same material.

Figure 19 represents the relationship between the birefringence coefficient $B/(1-f_0)$† (where f_0 is the porosity of the sample), which characterizes birefringence in the polymer constituent, and the thickness of the cellulose acetate films and specially prepared UAM ultrafiltration membranes of the same material. The figure shows perfect coincidence between the initial slopes of the $B/(1-f_0)$ vs H curves (which describe, according to Ref. [9], the degree of ordering in a polymer material) for membranes and films made on an adhesive support.

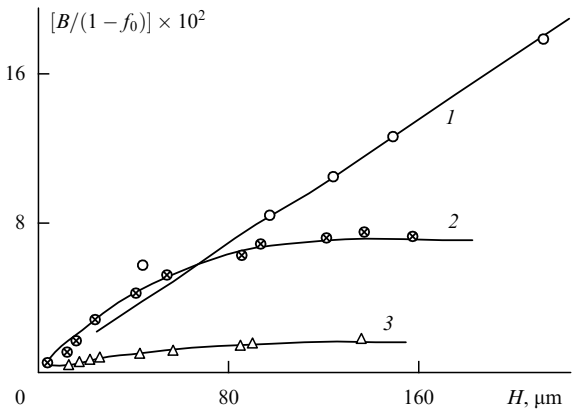

Figure 19. Dependence of the reduced birefringence coefficient $B/(1-f_0)$ on the thickness H for UAM-150 membranes (*1*) and cellulose acetate films on glass (*2*) and mercury (*3*) surfaces.

It follows that the polymer framework of ultrafiltration membranes possesses the same degree of planar ordering of macromolecular chains as polymer films formed on a solid support. However, planar ordering in membranes spreads over their entire volume [the straight line $B(H)$ remains linear up to the limiting value $H \approx 200$ μm], at variance with films in which oriented layers can be found not farther than 100 μm from the support (see above).

To illustrate this inference, Fig. 20 shows a typical micrograph of a thin section through a UAM-200 ultrafiltration membrane obtained in crossed nicols. It is readily seen that the polymer membrane is oriented throughout its volume unlike the dense cellulose acetate film in which the oriented layer is only about 100 μm thick (see Fig. 7).

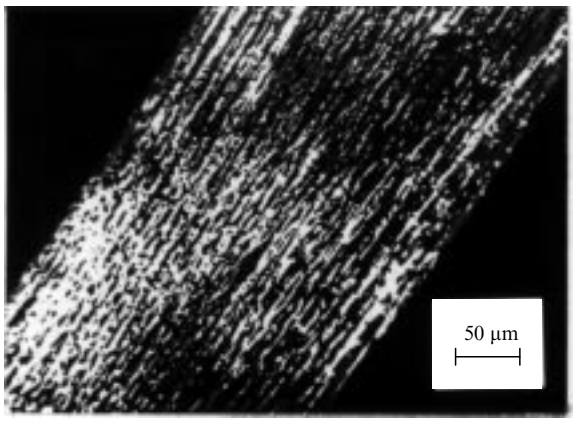

Figure 20. Micrograph of a thin section through a UAM-200 ultrafiltration membrane in crossed nicols.

The above data suggest the existence of a common ordering mechanism in membranes and films on solid supports. This suggestion was checked up in Ref. [48] by means of estimating the degree of orientational order which is likely to arise during membrane formation due to polymer gel shrinkage. The orientation process was simulated taking advantage of the Kargin – Shtending mechanism for the two-stage isotropic constriction – biaxial extension process assuming that it occurs in a glassy polymer. The value of $-S$ thus obtained lie in the 0.2 – 0.4 range, i.e. they are of the same order as typical S values for tightly packed films [9]. These estimates confirm the existence of a common ordering mechanism in membranes and films formed on solid supports. This mechanism accounts for thicker ordered layers in membranes arising from stronger intermolecular interactions in the polymeric milieu upon the addition of a precipitant.

The above observations pertain to membranes with isotropic structure. Studies of asymmetric membranes revealed the presence of birefringence indicative of planar ordering and birefringence of the opposite sign suggesting normal ordering in the polymer material. Solvent diffusion was reported to be accompanied by sign inversion of the birefringence which was ascribed by the authors to the reorientation of polymer segments under the influence of diffusive fluxes [49].

The effect of orientation processes on the structure of ultrafiltration membranes was examined in Ref. [50]. This paper describes consecutive simulations of membrane formation from cellulose acetate solutions in acetic acid using precipitants with various degrees of hardness. Precipitant hardness was adjusted by altering the concentration of aqueous acetic acid solutions from 15% (for soft precipitants) to 0% (for hard precipitants).

† The cofactor $(1-f_0)$ allows us to take into account the presence of pores which do not contribute to birefringence but occupy the relative volume f_0.

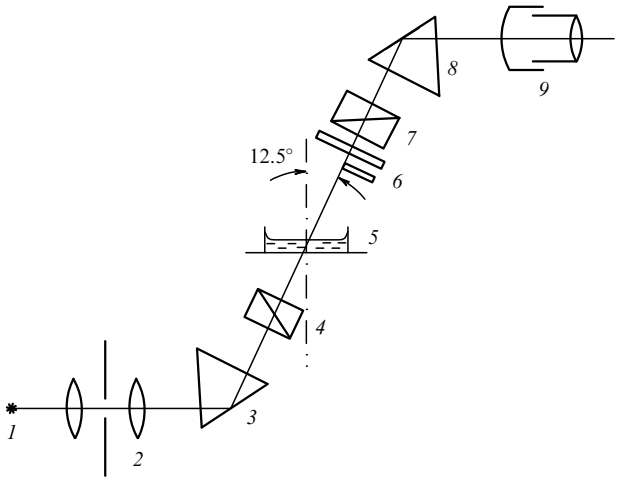

Figure 21. Schematic outline of the optical assembly for the examination of polymer solutions transmitting oblique incident light: *1* — light source, *2* — lenses, *4* and *7* — polarization prisms, *5* — polymer solution on a glass support, *6* — Breis' half-tone compensator, *3* and *7* — rotating prisms, *9* — eyepiece.

Birefringence was measured with a special device at a fixed angle of light transmission ($i = 12.5°$) through a polymer solution placed in a glass cuvette (Fig. 21).

The inherent anisotropy of cellulose acetate molecules is small [21], and the refractivity of the solvents used in this experiment is significantly different from the refractivity index of dry cellulose acetate. Therefore, the anisotropy of a monomer unit in this polymer depends solely on the effect of microform which is a positive value for anisodiametrical molecular structures. For this reason, the planar orientation of molecular fragments with respect to the support in a gel or solution must be reflected by a positive birefringence.

It turned out, however, that polymer solutions exhibit both positive and negative birefringence in the course of membrane formation. Figure 22 shows the birefringence at $i = 12.5°$ versus solvent evaporation time. It appears from Fig. 22 that the sign of birefringence undergoes inversion at the pre-casting stage (preliminary evaporation of the solvent before placing the sample into the precipitation tank). This suggests the alteration of the prevalent orientation patterns of molecular fragments relative to the substrate plane in the casting solution. Specifically, weak negative birefringence develops at the beginning of solvent evaporation which accounts for the predominant orientation of molecular chains perpendicular to the substrate surface. With the progression of evaporation, the sign of the birefringence changes which points to the largely planar orientation of molecular chains.

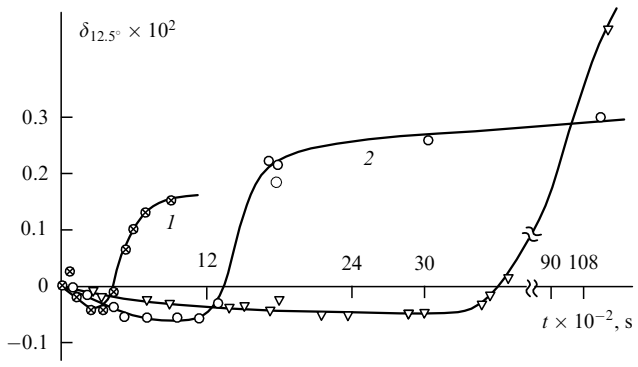

Figure 22. The relation between the birefringence $\delta_{12.5°}$ of a cellulose acetate solution in acetone and evaporation time for differing initial thicknesses of the layer: *1* — 50 μm, *2* — 100 μm, *3* — 200 μm (initial concentration 3%).

Figure 23 presents the dependence of birefringence on precipitation time in polymer solutions obtained by simulation of the second stage of membrane formation. As in the previous stage, immersion in the precipitant initiates competition between the two molecular orientation processes. However, the second stage differs from the first in that the prevalent orientation in the mature membrane depends on the precipitation conditions.

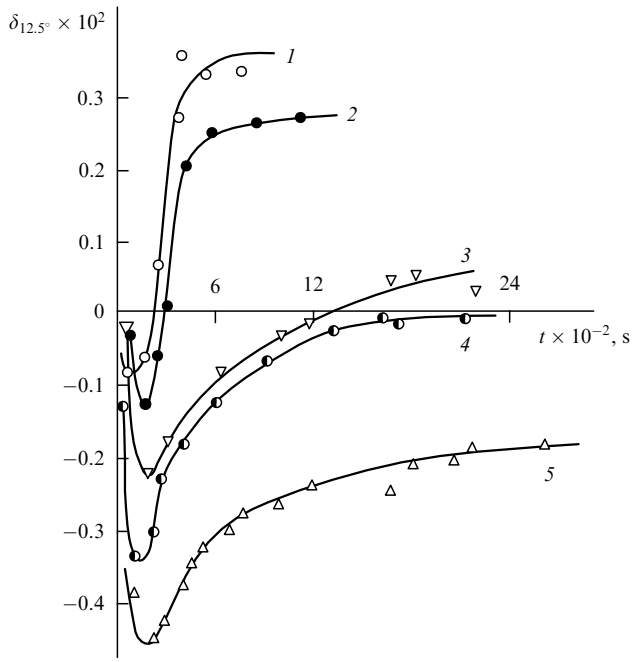

Figure 23. The relation between the birefringence $\delta_{12.5°}$ and the precipitation time for 3.5% cellulose acetate solutions using different precipitants: *1* — 15% acetic acid ($L_s = 150$ μm), *2* — 10% acetic acid ($L_s = 150$ μm), *3* — ice water ($L_s = 170$ μm), *4* — ice water ($L_s = 100$ μm), *5* — ice water ($L_s = 50$ μm).

Thus, the description of membrane formation in the experiment required the introduction of the concept of a 'normal' mechanism of orientation of chain fragments relative to the support, besides the planar polymer orientation concept. The possibility of 'normal' orientation may be due to the organizing effect of precipitant and solvent fluxes (see Ref. [52]).

The parallel action of two orientation mechanisms provides a qualitative explanation of membrane formation patterns.

Specifically, sedimentation of a polymer solution in the presence of a 'soft' precipitant (e.g. 15% or 10% acetic acid) is slow, and planar ordering that starts from the substrate has time to spread over the entire volume of the membrane (see Fig. 23 curves *1* and *2*). Conversely, in the presence of a 'hard' precipitant (ice water), the polymer precipitation front spreads from above and fixes the normal orientation pre-

existing in the solution. This restricts the planar order distribution to the layers immediately adjoining the substrate (curves *3*, *4*, and *5*). Therefore, the casting conditions for a polymer solution are responsible for the structural ordering in the membranes thus obtained.

The thickness of the solution (L_s) has a similar effect. An increase in L_s favors soft precipitation because diffusion of the precipitant into the depth of the solution results in its mixing with the solvent and a loss of rigidity. This preconditions the development of planar ordering in the bottom layers of the solution (curves *5*, *4*, and *3*). Subsequent precipitation of the previously oriented polymer accounts for the enhanced density of the layers showing planar ordering on the lower side of the polymer membranes.

Certain authors [24, 25, 51] explained the appearance of dense polymer layers on the lower membrane sides adjacent to the support by adsorption of polymer molecules at the substrate face followed by precipitation of these ordered layers. At the same time, evaluation of birefringence in solutions in which light passes at an angle to the support failed to reveal an appreciable orientation at the beginning of the process. The starting points of the curves in Figs 22 and 23 correspond to zero (within the limit of error). This questions the presence of more or less thick layers in adsorbed polymer solutions.

To summarize, analysis of polymer membrane production by angular BT has demonstrated the existence of mechanisms responsible for the formation of two types of ordered polymer materials. This analysis was carried out at the molecular level, but an additional study of isotropic membranes with the use of NMR spectroscopy has shown that the above mechanisms are equally operative at the macroscopic level, being responsible for the unique regularity of the filtering properties of membranes considered in this section.

6.3 Orientational order in the structure of polymer membranes

Refs [52, 53] report investigations of orientation in polymer membranes by the NMR technique. The local magnetic-field strength is known to be dependent on the size, shape, and orientation of the observed microvolumes, besides other factors. By representing a pore as an ellipsoid of revolution with the half-axes ratio x/y ($x \gg y$), the following expression was obtained for the magnetic-field strength (H) in a membrane pore:

$$H = H_0 \left\{ 1 + \frac{\Delta\chi}{4} \left[A_1 - A_2(\vartheta)(1 - \cos 2b) + A_3(\vartheta) \sin 2\varphi \right] \right\}, \tag{17}$$

where H_0 is the external field strength and $\Delta\chi$ is the difference between magnetic susceptibilities of polymeric and aqueous phases,

$$A_1 = 2(a^2 + b^2 - a^2 b^2)\,,$$

$$A_2 = \frac{1}{2}\left[3(a^2 + b^2 - a^2 b^2)\right],$$

$$A_3 = (1 - a^2)\cos\vartheta\,\overline{\cos 2\alpha} + \sin\vartheta\,\overline{\sin\beta}\,\sin 2\alpha\,,$$

$$a^2 = \overline{\cos^2\alpha} = \int_0^{2\pi} \cos^2\alpha\, f(\alpha)\,\mathrm{d}\alpha\,,$$

$$b^2 = \overline{\cos^2\beta} = \int_0^{2\pi} \cos^2\beta\, f(\beta)\,\mathrm{d}\beta\,.$$

Here, α and β are the pore orientation angles in the membrane, $f(\alpha)$ and $f(\beta)$ are the pore angular distribution functions at α and β, ϑ and φ are the membrane orientation angles in the magnetic field.

Therefore, for a membrane having several pore families with a predominant orientation at angles α and β, the magnetic field of each family will be given by expression (17) with functions A_1, A_2, and A_3, and the NMR spectrum will show several lines.

Studies of types MGA [52] and UAM isotropic cellulose acetate membranes and a nitrocellulose sartorius membrane (Germany) [53, 54] revealed two lines in the proton NMR spectrum (Fig. 24).

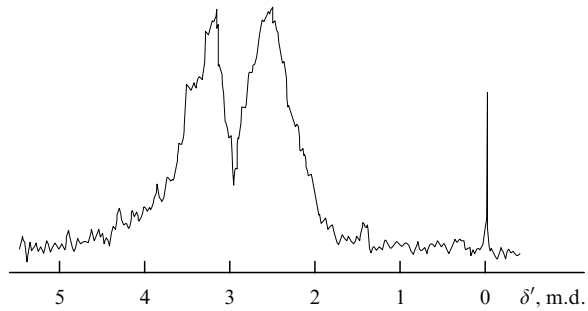

Figure 24. Aqueous proton spectrum in an isolated 150 μm thick UAM-150 membrane (δ' — chemical shift).

The orientation nature of the doublet was confirmed by the disappearance of the effect after the membrane was destroyed by pounding [52]. Moreover, an analysis of the angular dependence of the NMR spectrum gave evidence of a sinusoidal relationship between the chemical shift and the angle φ, in accordance with (17).

To conclude, the presence of two lines in the NMR spectrum corresponding to strong and weak fields respectively suggests the existence of two void systems in the membranes. Analysis of the temperature-dependence of chemical shifts indicates that the pores are arranged at the membrane plane and oriented normally to it [54]. By referring the spectral lines to planar and normal pores, the effective porosity of the membranes, i.e. the relative volume of working (normal) pores was evaluated. The areas under the peaks for two types of pores in the examined membranes are approximately the same, and the NMR signal is proportional to the number of observed nuclei. It is therefore possible to maintain that the working pore fraction in these membranes constitutes roughly half of the total volume.

7. Conclusion

Investigations into the structure and properties of surface layers are indispensable for the synthesis and modification of coatings, thin films, porous membranes, glues, composite materials, etc. Therefore, the development of new methods to study surface layers should be encouraged. The birefringence technique using polarized light that passes through a surface at an angle is an effective and highly sensitive tool for the characterization of polymer layers.

The present review describes the very first steps of the studies which are believed to be very promising bearing in mind that the properties of surface layers are crucial, and

sometimes determinant, for the physical and technical characteristics of thin films, fibers, membranes, and filled polymers.

Results obtained with the aid of this optical technique have demonstrated that surface orientational order is the result of both the polymer interaction with the support and the creation of the necessary kinetic conditions.

The fluctuation theory of polymer solidification that has recently been suggested by certain authors offers a qualitative explanation for the development of specific surface properties. This theory is based on the diffusion model of volume relaxation which accounts for the variation of the void volume by its diffusion towards the surface upon cooling of the polymer material, and back into the depth of the sample upon its heating. This means that cooling results in a diminished pore size or even their disappearance near the surface of polymer films due to the discharge of the pore void volume to the outside of the sample and the development of dense layers ('crusts') near the free surface. The total volume of these layers decreases while their area given by the sample size, remains unaltered. This causes a strong surface tension, and hence orientational order of both molecular fragments and supramolecular structures which make up the surface layer.

The mechanism of surface tension (i.e. void volume diffusion) is actually identical to the orientational order mechanism in films obtained by evaporation from polymer gels. 'Evaporation' of the void volume in the former case and of solvent molecules in the latter makes all the difference between the two mechanisms.

It is inferred from the results of experiments that the well-known beneficial effect of annealing on the quality of synthetic fibers is largely due to the orientation of structural elements in the surface layers. It appears that studies on filled polymer properties should be focused on orientational effects in surface layers of anisodiametrical filler particles and their influence on the major characteristics of polymer materials.

Certainly, this review does not pretend to offer any definitive solution; rather, it is intended to draw attention to the importance of investigations into the surface properties of polymer materials. We would like to emphasize the following issues that appear to be of special interest in this context: the use of angular BT to study evaporation kinetics in polymer film production, the effect of the film history on the optical properties of surface layers, surface birefringence in copolymers, block-copolymers, and other model polymers and dipole-containing polymers, birefringence in swollen polymer films during evaporation, surface optical anisotropy in uniaxially distorted films, the temperature-dependence of birefringence in surface layers and its contribution to the orientational order and behavior of molecular fragments and supramolecular structures in these layers.

References

1. Geguzin Ya E *Diffuzionnaya Zona* (Diffusion Zone) (Moscow: Nauka, 1979)
2. Bogdanova L M et a. *Dokl. Akad. Nauk SSSR* **268** (5) 1139 (1983) [*Sov. Phys. Dokl.*]
3. Bogdanova L M et al. *Vysokomol. Soedin. A* **26** (7) 1400 (1984)
4. Aleksandrov V N et al. *Vysokomol. Soedin. B* **27** (12) 914 (1985)
5. Rusanov A I *Fazovye Ravnovesiya i Poverkhnostnye Yavleniya* (Phase Equilibrium and Surface Phenomena) (Leningrad: Khimiya, 1967)
6. Askadskiĭ A A *Struktura i Svoĭstva Teplostoĭkikh Polimerov* (Structure and Properties of Thermoresistive Polymers) (Moscow: Khimiya, 1981)
7. Lipatov Yu S *Mezhfaznye Yavleniya v Polimerakh* (Interphase Phenomena in Polymers) (Moscow: Khimiya, 1980)
8. Irzhak B I, Rozenberg B A, Enikolopyan N S *Setchatye Polimery* (Polymer Networks) (Moscow: Nauka, 1979)
9. Cherkasov A N, Vitovskaya M G, Bushin S V *Vysokomol. Soedin. A* **18** (7) 1628 (1976)
10. Grishchenko A E et al. *Dokl. Akad. Nauk SSSR* **269** (6) 1384 (1983) [*Sov. Phys. Dokl.*]
11. Zhbankov R G, Tretinnikov O N, Tretinnikova G K *Visokomol. Soedin. B* **26** (2) 104 (1984)
12. Rostiashvilli V G, Irzhak V I, Rozenberg B A *Steklovanye Polimerov* (Solidification of Polymers) (Leningrad: Khimiya, 1987)
13. Ievlev V M, Trusov L I, Kholmyanskiĭ V A *Strukturnye Prevrashcheniya v Tonkikh Plenkakh* (Structural Transformations in Thin Films) (Moscow: Metallurgiya, 1988)
14. Povstugar V I, Kodolov V I, Mikhailova S S *Stroenie i Svoĭstva Poverkhnosti Polimernykh Materialov* (Surface Structure and Properties in Polymer Materials) (Moscow: Khimiya, 1988)
15. Stein R S *J. Pol. Sci.* **24** 383 (1957)
16. McNally J G, Sheppard S E *J. Phys. Chem.* **34** 165 (1930)
17. Matveenko V N, Kirsanov E A *Poverkhnostnye Yavleniya v Zhidkikh Kristallakh* (Surface Phenomena in Liquid Crystals) (Moscow: Izd. Mosk. Un-ta, 1991)
18. Deloche B, Samulski E *Macromolecules* **14** 575 (1981)
19. De Gennes P *Physics of Liquid Crystals* [Translated into Russian (Moscow: 1977)]
20. Grishchenko A E, Thesis for Doctorate of Physicomathematical Sciences (Siktivkar, Siktivkar Un-t, 1986)
21. Tsvetkov V N, Eskin V E, Frenkel' S Ya *Struktura Makromolekul v Rastvorakh* (Structure of Macromolecules in Solutions) (Moscow: Nauka, 1964)
22. Grishchenko A E et al. *Vysokomol. Soedin. A* **9** 1280 (1967)
23. Daletsky G F *Dokl. Akad. Nauk SSSR* **54** 313 (1946); **74** 685 (1950) [*C. R. Acad. Sci. URSS* **54** 311 (1946)]
24. Malinovsky Yu M *Usp. Khim.* **39** 1311 (1970)
25. Tanny G B *J. Appl. Pol. Sci.* **18** 2149 (1974)
26. Kargin V A, Shteding M N *Zh. Fiz. Khim.* **20** (7) 727 (1946)
27. Kozlov P V *Fiziko-khimiya Efirtselluloznikh Plenok* (Physico-Chemical Properties of Cellulose Ether Films) (Moscow: Goskinoizdat, 1948)
28. Grishchenko A E et al. *Vysokomol. Soedin. B* **27** (11) 814 (1985)
29. Bogdanova L M et al. *Vysokomol. Soedin. A* **29** (8) 1588 (1987)
30. Noshay A, McGrath J *Block Copolymers* [Translated into Russian (Moscow: 1980)]
31. Bjust J (Ed) *Polyurethane-Based Composite Materials* [Translated into Russian (Moscow: 1982)]
32. Kercha Yu Yu *Fizicheskaya Khimiya Poliuretanov* (Physical Chemistry of Polyurethanes) (Kiev: Naukova Dumka, 1979)
33. Lipatova T E *Vysokomol. Soedin. B* **29** (4) 255 (1987)
34. Turkov V K et al. *Vysokomol. Soedin. B* **30** (7) 499 (1988)
35. Turkov V K et al. *Vysokomol. Soedin. A* **32** (5) 1032 (1990)
36. Letunovsky M P et al. *Vysokomol. Soedin. A* **30** (2) 281 (1988)
37. Letunovsky M P et al. *Vysokomol. Soedin. A* **30** (2) 289 (1988)
38. Turkov V K et al. *Vysokomol. Soedin. A* **31** (1) 171 (1989)
39. Takahara A et al. *Polymer* **26** 978 (1985); **26** 987 (1985)
40. Turkov V K et al. *Vysokomol. Soedin. A* **30** (3) 640 (1988)
41. Skazka V S et al. *Vysokomol. Soedin. B* **26** (4) 295 (1984)
42. Grishchenko A E, Vorob'eva E P, Surkov V T *Vysokomol. Soedin. B* **17** (11) 820 (1975)
43. Kesting R E *Synthetic Polymeric Membranes* (New York: Wiley, 1985)
44. Bryk M T, Tsapyuk E A *Ul'trafil'tratsiya* (Ultrafiltration) (Kiev, Naukova Dumka, 1989)
45. Collins P *Fluid Flow Through Porous Materials* [Translated into Russian (Moscow: Mir, 1964)]
46. Cherkasov A N et al. *Izv. Akad. Nauk B. SSR Ser. Khim.* **1** 18 (1979)
47. Cherkasov A N et al. *Kolloid. Zh.* **43** (2) 382 (1981)
48. Cherkasov A N, Thesis for Doctorate of Physicomathematical Sciences (Leningrad: NTO AN SSSR, 1986)
49. Drechsel P, Hoard S L, Long F A *J. Pol. Sci.* **10** (2) 241 (1953)

50. Cherkasov A N, Tsareva S V *Plast. Massy* **1** 30 (1986)
51. Fujita S M, Soane D S *Pol. Eng. Sci.* **28** 341 (1988)
52. Mank V V, Kucheruk D D *Kolloid. Zh.* **35** (6) 1073 (1973)
53. Bizunok S N et al. *Vysokomol. Soedin.* **26** (5) 370 (1984)
54. Cherkasov A N et al. *Kolloid. Zh.* **43** (2) 382 (1981)
55. Magonov S N *Vysokomol. Soedin. B* **38** (1) 143 (1996)
56. Gallot B R *Adv. Polym. Sci.* **29** 85 (1978)
57. Gorelova M M et al. *Vysokomol. Soedin. A* **34** (2) 81 (1992)
58. Dolinniy A I, Ogorev V A *Usp. Khim.* **57** (11) 1769 (1988)
59. Lipatov Yu S, Alekseeva T T *Usp. Khim.* **61** (12) 2187 (1992)
60. Arslanov V V *Usp. Khim.* **61** (1) 3 (1994)
61. Sergeeva L M, Gorbach L A *Usp. Khim.* **65** (4) 367 (1966)
62. Parsonage E et al. *Macromolecules* **24** 1987 (1991)
63. Krivchenko et al. *Plast. Massy* **4** 26 (1988)
64. Kosyakov V I, Ginzburg L I *Diffuznye Yavleniya v Polimerakh* (Diffuse Phenomena in Polymers) (Chernogolovka: IKhF, 1985)
65. Akovali G, Biliyar K, Shen M *J. Appl. Pol. Sci.* **20** 2419 (1976)
66. Erukhimovich I Ya, Khokhlov A R *Vysokomol. Soedin. A* **35** (11) 1808 (1993)
67. Elsabee M Z, Dror M, Berry G C *J. Appl. Pol. Sci.* **28** 2151 (1983)
68. Grishchenko A E *Mekhanooptika Polimerov* (Mechanooptics of Polymers) (Peterburg.: Izd. Peterb. Un-t, 1966)